Check for updates

A comparison of acyl-moieties for noncovalent functionalization of PLGA and PEG-PLGA nanoparticles with a cell-penetrating peptide†

Omar Paulino da Silva Filho, [ab] Muhanad Ali,[c] Rike Nabbefeld,[a]
Daniel Primavessy, [de] Petra H. Bovee-Geurts,[a] Silko Grimm,[f] Andreas Kirchner,[d]
Karl-Heinz Wiesmüller, [g] Marc Schneider, [d] X. Frank Walboomers[c]
and Roland Brock [*ah]

Efficient intracellular drug delivery in nanomedicine strongly depends on ways to induce cellular uptake. Conjugation of nanoparticles (NPs) with cell-penetrating peptides (CPPs) is a known means to induce uptake *via* endocytosis. Here, we functionalized NPs consisting of either poly(D,L-lactide-*co*-glycolide) (PLGA) or polyethene glycol (PEG)-PLGA block-copolymer with a lactoferrin-derived cell-penetrating peptide (hLF). To enhance the association between the peptide and the polymer NPs, we tested a range of acyl moieties for N-terminal acylation of the peptide as a means to promote noncovalent interactions. Acyl moieties differed in chain length and number of acyl chains. Peptide-functionalized NPs were characterized for nanoparticle size, overall net charge, storage stability, and intracellular uptake. Coating particles with a palmitoylated hLF resulted in minimal precipitation after storage at −20C and homogeneous particle size (<200 nm). Palmitoyl-hLF coated NPs showed enhanced delivery in different cells in comparison to NPs lacking functionalization. Moreover, in comparison to acetyl-hLF, palmitoyl-hLF was also suited for coating and enhancing the cellular uptake of PEG-PLGA NPs.

1. Introduction

Polymeric nanoparticles (NPs) are versatile platforms for the incorporation of drugs and reporter molecules used in drug delivery and diagnostics.[1] Poly(lactic-*co*-glycolic acid) (PLGA) is one of the polymeric carrier materials approved by the FDA for use in humans.[2] PLGA is a hydrophobic polyester copolymer composed of different ratios of glycolic acid and lactic acid that can be confectioned into materials of different sizes and shapes.[3] Originally, PLGA was conceived for the fabrication of biomaterials due to its biocompatibility and biodegradability.[2] More recently, it has also been established as a drug delivery system, and submicron-size formulations have attracted interest in nanomedicine.[4]

In spite of its hydrophobic nature which favours the incorporation of hydrophobic drugs,[5] PLGA formulations encapsulating a broad spectrum of hydrophilic drugs or other compounds like peptides, proteins and nucleic acids have also been achieved.[6–8] Many nanomedicine applications share a requirement for cellular uptake, in particular in delivery of cancer drugs[9] and oligonucleotides.[10] However, PLGA particles by themselves have poor intracellular uptake. Therefore, various strategies have been devised to endow PLGA nanoparticles with functionalities that provide direct targeting to receptors and also enhance intracellular uptake,[11] such as coupling of cationic cell-penetrating peptides (CPPs).[12] The coupling strategies are based on covalent and noncovalent interaction.

For covalent functionalization diverse strategies using carbodiimide chemistry,[13–16] thiol-maleimide coupling,[17,18] and copper-catalyzed ligation have been presented.[19] Molecules can also be immobilized *via* non-covalent interactions. On one hand, cationic molecules, can be coated onto the surface of PLGA NPs through charge interactions with the anionic carboxyl group of PLGA chains.[20] On the other hand, making

[a]Department of Biochemistry, Radboud Institute for Molecular Life Sciences, Radboud University Medical Center, Geert Grooteplein 28, 6525 GA Nijmegen, The Netherlands. E-mail: roland.brock@radboudumc.nl

[b]CAPES Foundation, Ministry of Education of Brazil, DF, Brasília, 70.040-03, Brazil

[c]Department of Odontology and Biomaterials, Radboud University Medical Center, Nijmegen, The Netherlands

[d]Department of Biopharmacy and Pharmaceutic Technology, Saarland University, 66123 Saarbrücken, Germany

[e]Department of Pharmaceutics and Biopharmacy, Philipps-University Marburg, 35032 Marburg, Germany

[f]Evonik Industries, Health Care, Formulation and Polymers, Kirschenallee, 64293 Darmstadt, Germany

[g]EMC Microcollections GmbH, Sindelfinger Str. 3, 72070 Tübingen, Germany

[h]Department of Medical Biochemistry, College of Medicine and Medical Sciences, Arabian Gulf University, Kingdom of Bahrain

† Electronic supplementary information (ESI) available. See DOI: 10.1039/d1ra05871a

use of the hydrophobic nature of the PLGA,[5] acyl-modified peptides can be immobilized *via* hydrophobic interactions.[21]

Next to mediating cellular uptake, the pharmacological characteristics of PLGA can also be tuned by PEGylation, which prevents opsonization by serum proteins and thereby rapid clearance through uptake by the reticuloendothelial system.[22] Unless delivery exclusively relies on passive targeting by the enhanced permeation and retention (EPR) effect, PEGylation always acts in combination with strategies that mediate cell targeting and cellular uptake.[23]

Considering that noncovalent interactions circumvent the need for incorporation of functional groups, these can be considered the most straightforward strategy for surface modification of PLGA NPs. To our knowledge, so far a broader assessment of the dependence of surface functionalization and NP characteristics on the nature of the acyl chain has been missing. Here, we modified a lactoferrin-derived cell-penetrating peptide (hLF) with acyl chains of different lengths and different number of acyl moieties to address this question.

Interestingly, there was no explicit dependency on chain length. Overall, functionalization with palmitoyl (C16), C24 and a branched C20 moiety stood out in terms of preservation of PLGA particle size and stability. However, the palmitoylated peptide also yielded a stable, clear solution, while the other peptides precipitated over time. Importantly, the palmitoylated peptide also yielded functionalization of PEG-PLGA which provides an avenue for noncovalent modification of surface-shielded PLGA NPs.

2. Material and methods

2.1. Peptides

All peptides were synthesized as C-terminal amides by EMC microcollections (Tübingen, Germany) using solid-phase peptide synthesis. For efficient disulfide bridge formation, hLF peptides were dissolved in 50 mM Hepes buffer pH 8 at a concentration of 2 mM and oxidized for 2 hours at 37 °C.[24]

2.2. Particle preparation

2.2.1. Preparation of FA-PLGA nanoparticles loaded with rhodamine-B dextran by double emulsion solvent diffusion. Rhodamine-B Dextran (10 000 MW) was obtained from Life Technologies (Darmstadt, Germany). Fluoresceinamine-PLGA (FA-PLGA) was made by coupling fluoresceinamine (Life Technologies, Darmstadt, Germany) and PLGA (Resomer RG 503H, Evonik Industries, Darmstadt, Germany), using a previously described method.[25,26] For particle preparation, 50 mg of FA-PLGA was dissolved in 1.5 mL of ethyl acetate (Sigma Life Science, Zwijndrecht, the Netherlands). Rhodamine-B dextran was dissolved in Milli-Q water at a concentration of 2 mg mL^{-1}. 0.5 mL of rhodamine-B dextran solution was added to the dissolved FA-PLGA. A (primary) w/o emulsion was prepared by sonication at approximately 6 W for one minute. Then, 2.5 mL of a 25 mg mL^{-1} PVA (MW 9000–10 000, 80% hydrolyzed) (Sigma Life Science, Zwijndrecht, the Netherlands) aqueous solution was added to the emulsion. The mixture was again

sonicated at approximately 15 W for 60 seconds resulting in a secondary emulsion. The volume of this emulsion was increased to 20 mL by adding Milli-Q water. Upon volume increase, the ethyl acetate in the emulsion drops exceeded the non-miscibility border of the two partially soluble solvents and rhodamine-B dextran loaded FA-PLGA NPs precipitated from the emulsion. The sample was then freeze-dried.

2.2.2. Preparation of PEG-PLGA nanoparticles loaded with BODIPY by double emulsion solvent diffusion. PEG-PLGA NPs loaded with 4,4-difluoro-4-bora-3*a*,4*a*-diaza-*s*-indacene (also known as boron dipyrrolylmethene, hereafter abbreviated to BODIPY) 500/510 C1, C12 (Thermo Fisher Scientific, Breda, the Netherlands) was encapsulated into Resomer select 5050DLC mPEG 5000 (15 *w*% PEG) (Evonik Industries) by the double emulsion solvent diffusion method. For particle preparation, 50 mg of PEG-PLGA was dissolved in 1.5 mL of ethyl acetate. BODIPY was dissolved in 80% ethanol at a concentration of 100 μg mL^{-1} and 0.05 mL added to the dissolved PEG-PLGA. A (primary) w/o emulsion was prepared by sonication at approximately 50 W for one minute. Then, 2.5 mL of a 25 mg mL^{-1} PVA (MW 9000–10 000, 80% hydrolyzed) solution, containing 1% penicillin/streptomycin, was added to the formulation. Next, the material was vortex mixed and sonicated at approximately 50 W for 60 seconds resulting in a secondary emulsion. The organic solvent was removed using a rotary evaporator Rotavapor R-100 (Buchi, Postfach, Switzerland) and the sample was washed three times using a 100 kDa cut-off filter (Amicon ultra-15 centrifugal filter unit, Millipore, Amsterdam, the Netherlands). Washed samples were spun down at 8000*g* for 20 min at 4 °C and freeze-dried.

2.2.3. Preparation of rhodamine-B-ethylenediamine-PLGA nanoparticles by single emulsion solvent diffusion. Lissamine rhodamine-B-ethylenediamine was obtained from Life Technologies and covalently coupled to PLGA (Resomer RG 503H) using a method described elsewhere[26] for fluoresceinamine and PLGA with minor changes. 50 mg of rhodamine-B PLGA (RhB–PLGA) was dissolved in 1.5 mL ethyl acetate. Then 2.5 mL of a 25 mg mL^{-1} PVA (MW 9000–10 000, 80% hydrolyzed) aqueous solution was added, and the mixture was sonicated at approximately 16 W for one minute. The volume of the resulting emulsion was increased to 20 mL by adding Milli-Q water. After this procedure, the sample was freeze-dried.

2.2.4. Freeze-drying. The PLGA particle suspensions were aliquoted in 5 mL quantities and put into 15 mL tubes. For each 5 mL, 150 mg D-sorbitol (Sigma Aldrich, Taufkirchen, Germany) was added. The tubes were frozen at − 80 °C for at least three hours and then lyophilized for at least three days.

2.2.5. Surface functionalization of nanoparticles. Before noncovalent coating of the particles with the peptides, the PLGA particles were washed once with Milli-Q water to remove remaining ethyl acetate, sorbitol and PVA. The washing step consisted of centrifuging particles at 16 000*g* for 10 min at 4 °C and resuspending the particles in Milli-Q water. A 100 μL colloidal solution containing 2.5 mg mL^{-1} particles and 0.1 mg mL^{-1} peptides diluted in Milli-Q water (10-fold dilution factor) was incubated overnight, in the cold room, on a roller mixer. To

remove the unbound peptides after the coating, the particles were washed.

2.3. Dynamic light scattering

Size and zeta potential measurements were performed on a Zetasizer Nano S, using a 633 nm HeNe laser with 4 mW (Malvern Panalytical, Malvern, UK). Particles were diluted to a concentration of 0.25 mg mL^{-1} in Milli-Q water. For size and zeta potential, three measurements were performed per sample with an automatic selection for the number of runs. For size measurements, the backward scatter was used. Data analysis was carried out with ZetaSizer software 7.03.

2.4. Cell culture

HeLa cells were obtained from the German Collection of Microorganisms and Cell Cultures (DSMZ, Braunschweig, Germany) and were cultivated in RPMI containing 10% fetal calf serum (FCS, Gibco). Caco-2 cells were a kind gift from Fraunhofer IGB (Stuttgart, Germany) and were cultured in MEM containing 20% FCS, 1% non-essential amino acids and 1% sodium pyruvate. All cell culture materials were purchased from Invitrogen (Carlsbad, US). Human periodontal ligament cells (PDLCs) were used following national guidelines for working with human materials (Dutch Federation of Biomedical Scientific Societies, human tissue and medical research: code of conduct for responsible use).[27] The cell proliferation medium consisted of advanced Dulbecco's Modified Eagle Medium/Ham's F-12 (DMEM/F-12, Gibco) supplemented with 10% fetal calf serum and 1% penicillin/streptomycin (Gibco). PDL cells were cultured for a total of three passages and then frozen in medium supplemented with 10% dimethyl sulfoxide (Sigma) in liquid nitrogen. After defrosting, cells from the 5th passage were used.

2.5. Confocal laser scanning microscopy

HeLa, Caco-2, and PDL cells were seeded one (40 000 cells) or two days (20 000 cells) before the experiment in Nunc (Wiesbaden, Germany) or ibidi (Martinsried, Germany) 8-well coverslip-bottom microscopy chambers. Cells were incubated for 2 hours with 250 μL of a 0.4 mg mL^{-1} PLGA particle solution, in RPMI containing 10% FCS. HeLa cells and PDL cells were also incubated for 2 hours with 250 μL of a 1.2 mg mL^{-1} PEG-PLGA NP solution functionalized with acylated peptides. Before imaging, cells were washed twice with media and incubated for 20 min with 250 μL of 1 μg mL^{-1} Hoechst 33342 (Thermo Fisher Scientific) and a 5 μg mL^{-1} CellMask Deep Red plasma membrane stain solution (Thermo Fisher Scientific). Each well was then rinsed twice before imaging. Images were collected using a TCS SP5 confocal microscope (Leica Microsystems, Mannheim, Germany) equipped with an HCX PL APO 63 × 1.2 water immersion lens. Hoechst 33342 was excited at 405 nm and emission collected between 461 and 500 nm. Fluorescein and Bodipy were excited with the 488 nm laser line of an argon-ion laser and the emission collected between 500 and 550 nm. Rhodamine-Dextran was excited with a 561 nm laser and emission collected between 570 and 620 nm. CellMask

Deep Red plasma membrane stain was excited with a 633 nm laser and emission collected between 666 and 710 nm. For the imaging of two or more colours, sequential scanning was used to avoid overlap of the emission spectra.

2.6. Flow cytometry

20 000 HeLa and PDL cells were seeded per well in a 96-well plate (Corning, Kennebunk, USA) one day before the experiment. Cells were incubated for 2 hours with 100 μL solution containing 0.4 mg mL^{-1} particles, diluted in serum-containing medium followed by washing and trypsinization for 5 min at 37 °C. Detached cells were resuspended in phenol-red free RPMI containing 10% FCS. After resuspension, the cell-associated fluorescence was measured using a MACSQuant flow cytometer (Miltenyi Biotec, Leiden, the Netherlands). Analysis of 10 000 gated cells was performed using FlowJo software (Franklin Lakes, NJ, USA).

2.7. Cell viability assay

20 000 HeLa cells were seeded one day prior to incubation with nanoparticles in 96-well plates. Cells were incubated for 24 hours with the indicated particle concentrations in RPMI + 10% FCS. Cells were washed twice with medium and 100 μg mL^{-1} resazurin (Sigma-Aldrich) dissolved in RPMI + 10% FCS were added. 50% DMSO was used as a negative control for cell viability. After incubating cells for 2 hours, fluorescence was measured using a BioTek Synergy 2 plate reader (excitation: 540 nm, emission: 620 nm). Autofluorescence of resazurin was subtracted from all samples, and the percentage of viable cells was determined by setting the untreated cells to 100%.

3. Results

Noncovalent interactions provide the most straight-forward means to equip nanoparticles with additional functionalities. However, it has to be ensured that the coupling is of sufficient strength to minimize leakage of the functionality and that functionalization maintains the stability and monodispersity of the particles. Here, we explored the impact of acylation of the lactoferrin-derived cell-penetrating peptide (hLF) with acyl chains with different length and number on the noncovalent functionalization of PLGA particles.

3.1. Characterization of the hLF-coated PLGA particles

First, we identified the experimental conditions for the preparation and characterization of hLF-coated PLGA NP using acetyl-hLF. When comparing peptide concentrations of 1, 0.1 and 0.01 mg mL^{-1} we noted that at 0.01 mg mL^{-1} no reversal of zeta potential from negative to positive values was achieved and that 0.1 mg mL^{-1} was sufficient to yield a positive zeta potential also after particles were washed and stored for up to three days (ESI Fig. S1†). In addition, for the 0.1 mg mL^{-1} hLF coated NPs, the zeta potential was slightly higher after overnight incubation compared to one-hour incubation. Therefore, the overnight coating was used as the method of choice for all following experiments. A BCA assay (see ESI† methods) was performed to

estimate the amount of hLF adsorbed onto the nanoparticle surface. Approximately one-third of the peptides present in the incubation solution (33 ± 4 µg mL^{-1}) remained attached to the particles after one day of incubation (ESI Fig. S2†). Another essential issue to take into account was the storage of the particles. We decided to store the particles in buffered solution to ensure a stable pH and thereby prevent acidification through degradation of PLGA (ESI Fig. S3†).

In order to identify an optimal acyl moiety for noncovalent immobilization of the hLF peptide on PLGA NPs, the hLF peptide was N-terminally extended with mono-acyl chains of different length (C8, C12, C16, C20, C24, C28) (Fig. 1). In addition, we also tested branched ($2 \times C_n$) acyl chains by coupling two fatty acid chains (C16, C20, C24, C28) linked via a glycerol backbone. Finally, we included a mycolyl moiety which is similar to the $2 \times C16$ with the only difference being the linkage between the two acyl chains.

We used two types for formulations, namely rhodamine-dextran loaded and fluorescein-conjugated PLGA (FA-PLGA), and rhodamine-conjugated PLGA. The dual labelled particles were intended to enable a distinction between cellular uptake of polymer and cargo. First, the particles were characterized with regard to size, batch heterogeneity (also known as polydispersity index, PDI), and overall net charge (zeta potential). For the rhodamine-dextran FA-PLGA particles, coating with hLF with acyl chains up to C16 fully preserved particle size and monodispersity, also over a period of up to eight days. The same was true for the mycolyl residue and the bis-C20 moiety (Fig. 2). The other peptides led to aggregation, either from the onset on or over time. Size always increased together with polydispersity, indicating that the average size changed because of aggregation and not because of a change of particle characteristics. Acylation promoted the association of the hLF peptide with the particles as indicated by the more positive and also more stable zeta-potentials over time. The rhodamine-conjugated PLGA

particles had a stronger tendency to aggregate (Fig. 2D, E and ESI Fig. S4B†). In this case, C24 showed the most favorable characteristics in terms of maintenance of stability and zeta potential. However, also the peptides by themselves differed in their tendency to aggregate. While peptides with C16 or mycolyl acyl chains formed stable solutions, peptides with a longer acyl chain and the bis-acylated peptides ($2 \times C28$, $2 \times C24$, $2 \times C20$, C28, C24, and C20) precipitated after storage, (ESI Fig. S5†).

3.2. Interaction of hLF-coated PLGA particles with cells

C16-, C24- and mycolyl-acylations had shown superior characteristics with respect to particle coating and preservation of particle size. Next, we investigated cellular association and uptake for nanoparticles functionalized with the whole set of peptides. In order to discriminate between the particles themselves and the cargo, PLGA was covalently labelled with fluorescein (FA-PLGA) and loaded with rhodamine-dextran. Due to coupling to the dextran polymer, the rhodamine did not leak out of the particles (ESI Fig. S6†). By comparison for NPs loaded with 6-coumarin and fluorescein, the fluorescent cargo leaked out of the particles (ESI Fig. S6†). These double-labelled particles were compared again with particles in which the PLGA was covalently conjugated to rhodamine. Following incubation of HeLa and Caco-2 cells with the labelled particles for 2 hours the uptake was analyzed with confocal microscopy.

Particles coated with acylated hLF variants showed a stronger association with cells and also a higher uptake than the control acetyl-hLF-coated particles (Fig. 3A, B, ESI Fig. S7 and S8†). At the 2 hour time point most particles were still localized on the cell surface, but uptake of particles had also occurred (ESI Fig. S9†). Importantly, the incubation with hLF-coated PLGA NPs did not cause toxicity (ESI Fig. S10†). Also for the rhodamine-PLGA particles, the acylated variants showed a stronger uptake than the particles coated with acetyl-hLF (Fig. 3C). Coated particles showed similar cell association 2
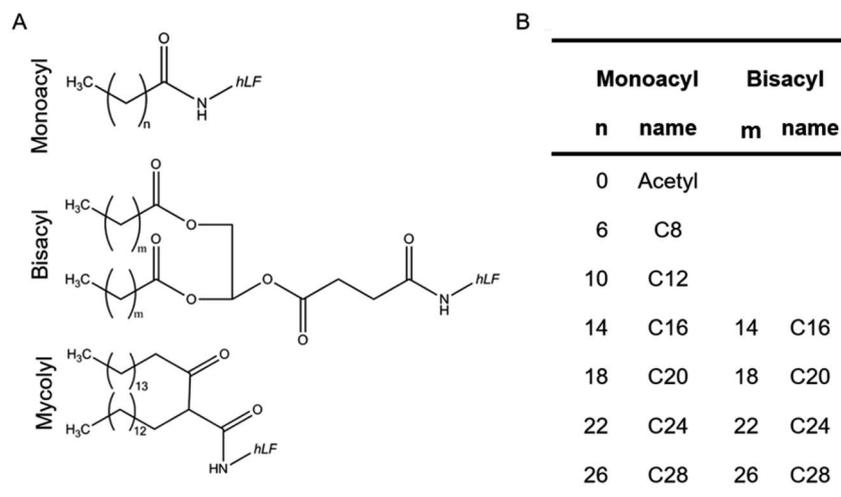

Fig. 1 Structures of the acylated hLF peptides tested. (A) Monoacyl-, bisacyl-, and mycolyl, moieties with (B) different carbon lengths (respectively n or m) were coupled to the N-terminus of hLF. The amino acid sequence of the hLF peptide is KCFQWQRNMRKVRGPPVSCIKR−NH$_2$ where −NH$_2$ stands for C-terminal amidation.

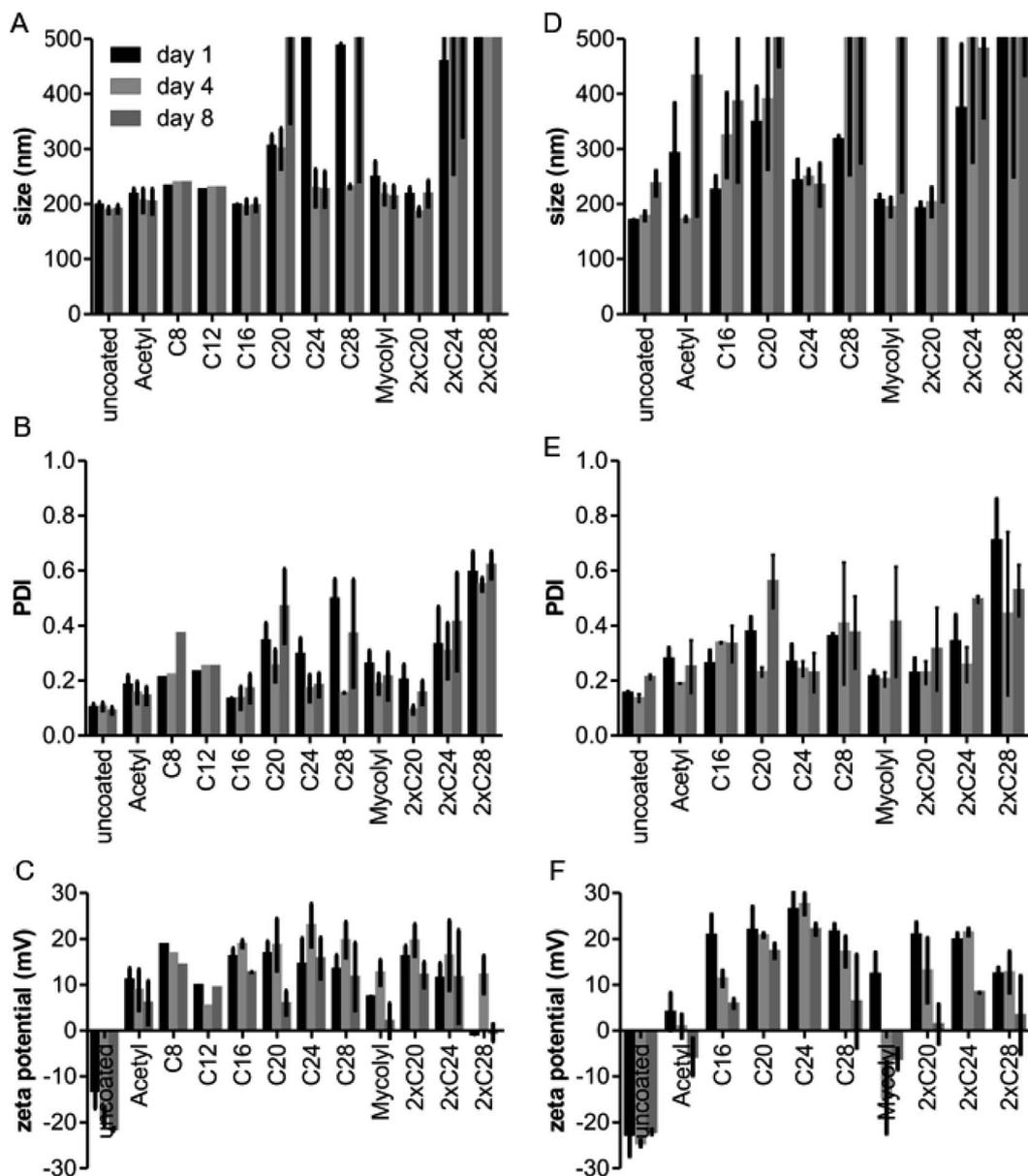| Monoacyl		Bisacyl	
n	name	m	name
0	Acetyl		
6	C8		
10	C12		
14	C16	14	C16
18	C20	18	C20
22	C24	22	C24
26	C28	26	C28

Fig. 2   Time-dependence of size, polydispersity and zeta potential of PLGA particles coated with acylated hLF peptides. (A–C) Rhodamine-dextran-loaded fluorescein-conjugated PLGA (FA-PLGA) and (D–F) rhodamine-conjugated PLGA particles were prepared in water and coated with 0.1 mg mL^{-1} peptide overnight at RT. Size, polydispersity index (PDI) and zeta potential were assessed after coating, at day one, four and eight. Technical replicate $N = 1$ for C8 and C12, $N = 3$ for uncoated, acetyl, C16, C24 and mycolyl in FA-PLGA rhodamine-dextran particles, for all other samples $N = 2$.

hours after incubation (day 1), and uptake was also observed for particles that had been stored for 7 days (ESI Fig. S7†). By combining all data (maintenance of monodispersity, the stability of coating, cellular activity and solubility), we decided to further use palmitoyl-hLF as the analog with the most favourable characteristics.

3.3.   Acylated PEG-PLGA nanoparticles

Nanoparticles in circulation are rapidly opsonized and cleared by the reticuloendothelial system (RES). To avoid opsonization and extend circulation time, coating of nanoparticles with polyethylene glycol (PEG) is a well-established method.[28] Since

PEGylation is considered to impose a general barrier to an association of molecules, we wanted to learn whether the acylated peptides could nevertheless be used for functionalization of nanoparticles and enhance cellular uptake. Here, C16-hLF was employed as the acylated analogue with the most favourable characteristics. For uptake assays using PEG-PLGA NPs, BODIPY was used as model drug, due to its fluorescence and hydrophobic characteristics.[29,30] Incubation of BODIPY-loaded PEG-PLGA NPs with acetyl-hLF and C16-hLF increased the zeta potential from −22.96 mV to 4.5 mV and 19.3 mV, respectively (ESI Fig. S11†). C16-hLF coated PEG-PLGA particles outperformed acetyl-hLF and uncoated particles when delivered
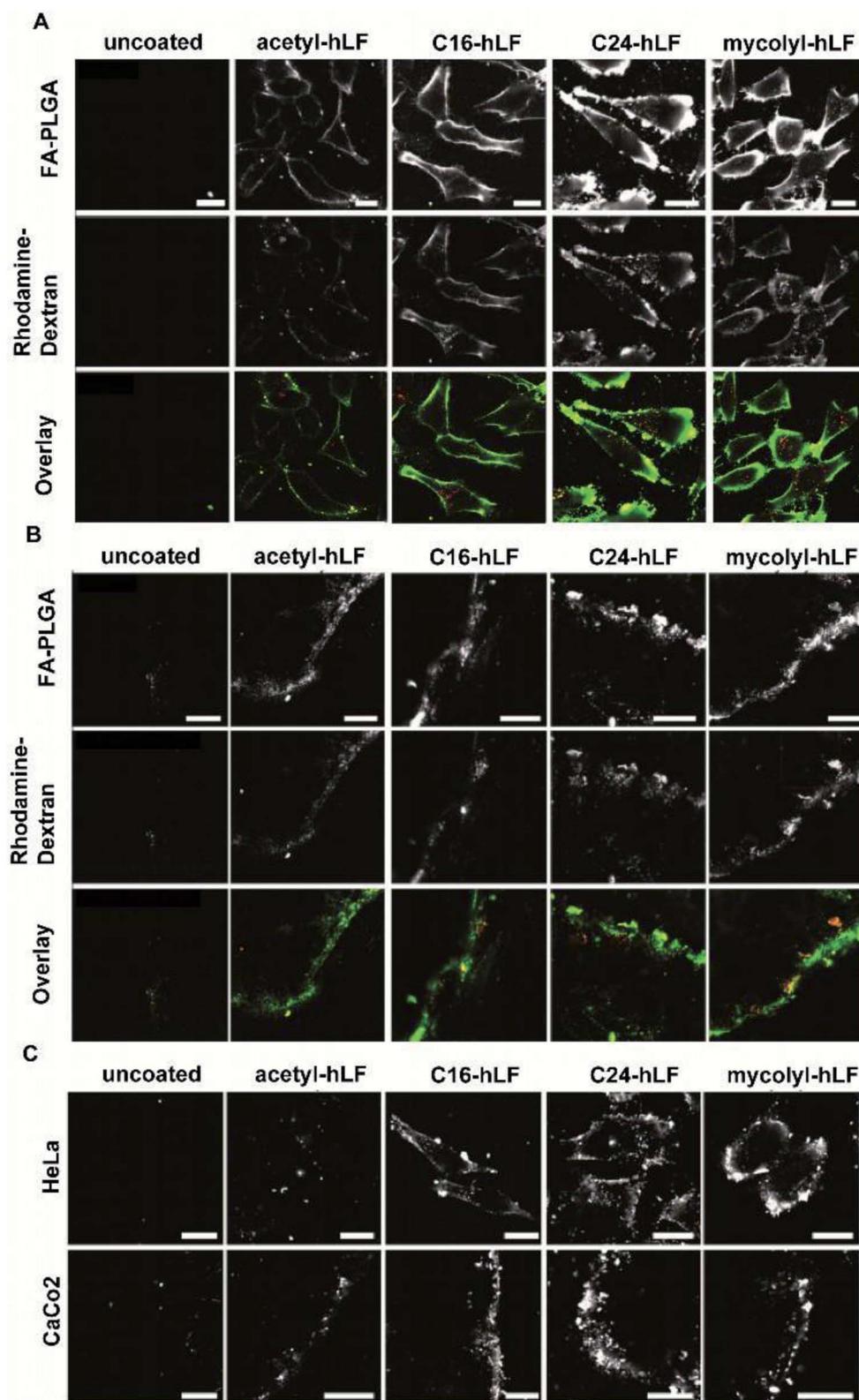
Fig. 3 Confocal microscopy of labelled PLGA nanoparticles. (A) HeLa and (B) Caco-2 cells were incubated with the peptide-coated fluorescein-conjugated PLGA (FA-PLGA) rhodamine-dextran particles. (C) HeLa and Caco-2 cells were incubated with the peptide-coated rhodamine-PLGA particles. Incubation was performed at a PLGA concentration of 0.4 mg mL^{-1} for 2 hours at 37 °C. Scale bar represents 20 μm. Green: FA-PLGA; red: rhodamine-Dextran.

to different cell lines (Fig. 4A and B). Next, we observed that C16-hLF coated PEG-PLGA NPs were internalized by HeLa (Fig. 4C) and periodontal ligament (PDL) cells (ESI Fig. S12†). Primary PDL cells are responsible for periodontal homeostasis and regeneration,[31,32] serving as a clinical target for the treatment of periodontal disease and drug delivery strategies based on PLGA nanoparticle formulations.[33]

4. Discussion

Here, we showed that the functionalization of anionic PLGA NPs with a cationic CPP can be improved by acylating the peptide. There were pronounced differences with respect to maintenance of monodispersity and coating in dependence of acyl chain length and structure. Importantly, this capacity could also be extended to PEG-PLGA particles.

Particle size and overall net charge (zeta potential) were used as read-outs to evaluate the efficiency of peptide coating for PLGA and PEG-PLGA NPs. C16- and mycolyl-hLF-coated particles were the most stable and retained functionalization in solution over several days.

To our knowledge, this is the first time that PLGA and PEG-PLGA nanoparticles were successfully functionalized with an acylated cationic cell-penetrating peptide by noncovalent interactions. So far, the concept of lipid anchors to decorate nanoparticles has been primarily explored for liposomes.
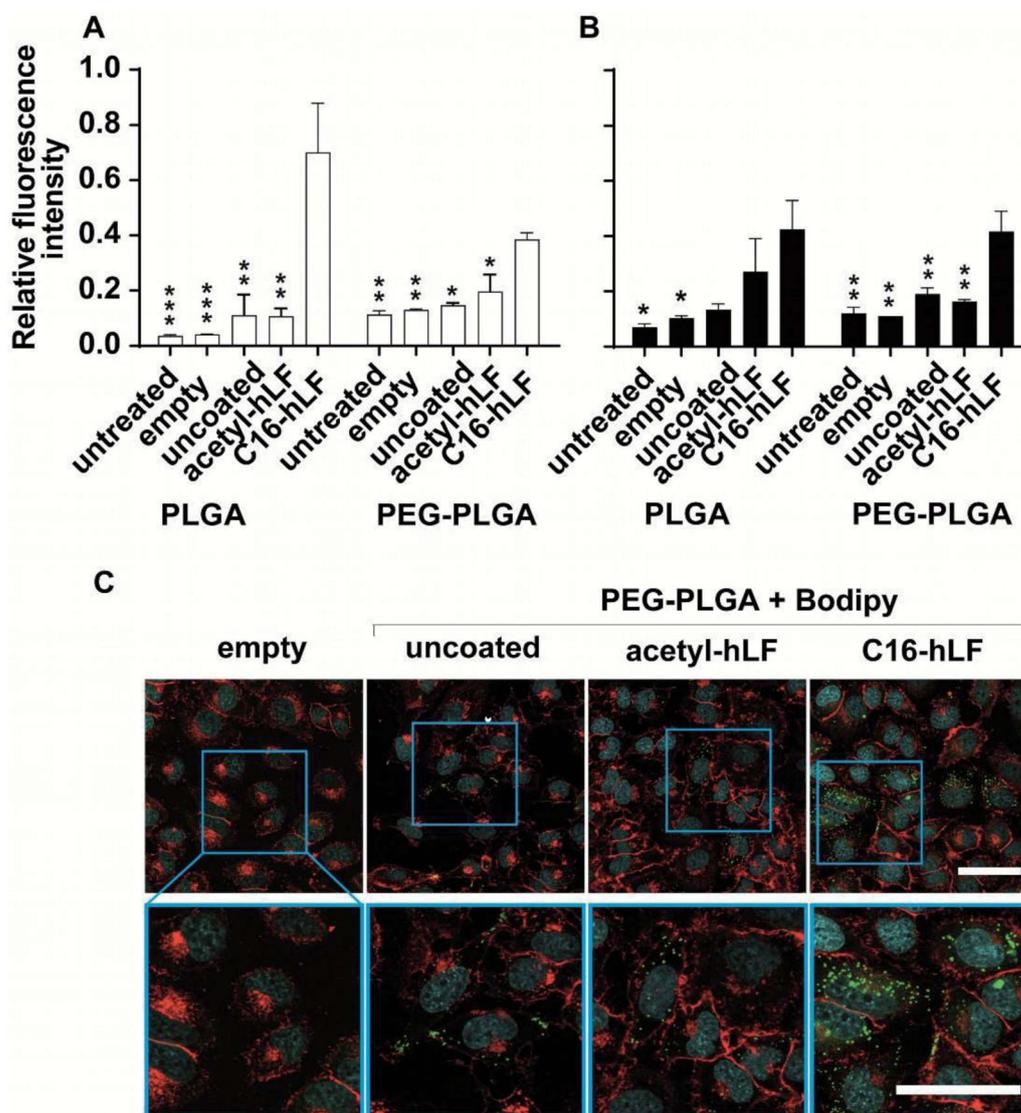
Fig. 4 Preferential uptake of C16–hLF-coated PEG-PLGA particles. Flow cytometry of (A) HeLa and (B) periodontal ligament cells incubated with peptide-coated particles for 2 hours at 37 °C. Shown are relative fluorescence intensities. The average of four technical replicates of two independent experiments was normalized to the sum of all means and are represented as means ± SEM. The multiple comparisons of the significance of differences between the C16–hLF-coated nanoparticles and the tested samples were determined using one-way ANOVA. Significance values shown in graphs from Tukey's multiple comparison test (ns $P > 0.05$, *$P ≤ 0.05$, **$P ≤ 0.01$, ***$P ≤ 0.001$). (C) HeLa cells incubated with Bodipy-loaded PEG-PLGA particles for 2 hours at 37 °C. Red: cell mask; cyan: Hoechst 33342; green: BODIPY. Blue squares represent the area in which pictures were enlarged (bottom panels). Scale bar represents 50 μm.

Lipidated polyarginine CPPs have been anchored in the surface of lipid nanoparticles, improving drug delivery properties of liposomes without[34] or with additional coating strategies as for example PEG.[35,36]

Noncovalent functionalization of PLGA nanoparticles is a significant advancement in the field of drug delivery as the focus so far has been directed towards covalent functionalization.[37] Covalent surface functionalization of PLGA nanoparticles can be difficult because this aliphatic polyester only offers a low reactivity functionalization site at the hydroxyl side-chains of the backbone. Therefore, multi-step approaches focus on the uncapped ends of the PLGA chains, where the available carboxylic acid groups can be employed for conjugation reactions, as described.[12,13,17,18]

Positively charged CPPs can exploit electrostatic interactions of the cationic amino acid side chains with the negatively charged PLGA to decorate the NPs surface.[20] However, as we demonstrate the noncovalent functionalization using CPPs can be improved when using a lipid anchor (acylated peptides), ultimately improving PLGA and PEG-PLGA NPs uptake in different cell lines. In spite of the overall shielding characteristic of the PEG layer, the acylated peptides associated with the particles and this association was stronger for the C16-acylated peptide than for the acetylated one. The functionalization of PEGylated nanoparticles with acyl-anchored peptides is a significant step for direct NP functionalization without using the PEG moiety as a spacer between the NPs surface and the functional peptide. Evidently, also in the context of the PEG layer the CPP exerts its function.

Conflicts of interest

R. Brock is inventor on a patent (US 2013/0108662 A1) related to the use of human lactoferrin-derived cell-penetrating peptides.

Acknowledgements

References

1 I. Ekladious, Y. L. Colson and M. W. Grinstaff, Polymer-drug conjugate therapeutics: advances, insights and prospects, *Nat. Rev. Drug Discovery*, 2019, **18**(4), 273–294.

2 K. Park, *et al.*, Injectable, long-acting PLGA formulations: Analyzing PLGA and understanding microparticle formation, *J. Controlled Release*, 2019, **304**, 125–134.

3 D. Ding and Q. Zhu, Recent advances of PLGA micro/nanoparticles for the delivery of biomacromolecular therapeutics, *Mater. Sci. Eng., C*, 2018, **92**, 1041–1060.

4 E. Swider, *et al.*, Customizing poly(lactic-*co*-glycolic acid) particles for biomedical applications, *Acta Biomater.*, 2018, **73**, 38–51.

5 C. Wischke and S. P. Schwendeman, Principles of encapsulating hydrophobic drugs in PLA/PLGA microparticles, *Int. J. Pharm.*, 2008, **364**(2), 298–327.

6 D. Essa, *et al.*, The Design of Poly(lactide-co-glycolide) Nanocarriers for Medical Applications, *Front. Bioeng. Biotechnol.*, 2020, **8**, 48.

7 F. Ramazani, *et al.*, Strategies for encapsulation of small hydrophilic and amphiphilic drugs in PLGA microspheres: State-of-the-art and challenges, *Int. J. Pharm.*, 2016, **499**(1–2), 358–367.

8 D. Primavessy, N. Gunday Tureli and M. Schneider, Influence of different stabilizers on the encapsulation of desmopressin acetate into PLGA nanoparticles, *Eur. J. Pharm. Biopharm.*, 2017, **118**, 48–55.

9 S. Senapati, *et al.*, Controlled drug delivery vehicles for cancer treatment and their performance, *Signal Transduction Targeted Ther.*, 2018, **3**, 7.

10 R. L. Setten, J. J. Rossi and S. P. Han, The current state and future directions of RNAi-based therapeutics, *Nat. Rev. Drug Discovery*, 2019, **18**(6), 421–446.

11 M. A. Holgado, *et al.*, Possibilities of poly(D,L-lactide-co-glycolide) in the formulation of nanomedicines against cancer, *Curr. Drug Targets*, 2011, **12**(8), 1096–1111.

12 I. Gessner and I. Neundorf, Nanoparticles Modified with Cell-Penetrating Peptides: Conjugation Mechanisms, Physicochemical Properties, and Application in Cancer Diagnosis and Therapy, *Int. J. Mol. Sci.*, 2020, **21**(7), 2536.

13 L. Costantino, *et al.*, Peptide-derivatized biodegradable nanoparticles able to cross the blood–brain barrier, *J. Controlled Release*, 2005, **108**(1), 84–96.

14 G. Tosi, *et al.*, Targeting the central nervous system: *in vivo* experiments with peptide-derivatized nanoparticles loaded with Loperamide and Rhodamine-123, *J. Controlled Release*, 2007, **122**(1), 1–9.

15 Z. Wang, W. K. Chui and P. C. Ho, Nanoparticulate delivery system targeted to tumor neovasculature for combined anticancer and antiangiogenesis therapy, *Pharm. Res.*, 2011, **28**(3), 585–596.

16 S. Streck, *et al.*, The distribution of cell-penetrating peptides on polymeric nanoparticles prepared using microfluidics and elucidated with small angle X-ray scattering, *J. Colloid Interface Sci.*, 2019, **555**, 438–448.

17 U. S. Toti, *et al.*, Interfacial activity assisted surface functionalization: a novel approach to incorporate maleimide functional groups and cRGD peptide on polymeric nanoparticles for targeted drug delivery, *Mol. Pharm.*, 2010, 7(4), 1108–1117.

18 L. Martinez-Jothar, *et al.*, Insights into maleimide-thiol conjugation chemistry: Conditions for efficient surface functionalization of nanoparticles for receptor targeting, *J. Controlled Release*, 2018, **282**, 101–109.

19 J. Lu, M. Shi and M. S. Shoichet, Click chemistry functionalized polymeric nanoparticles target corneal

epithelial cells through RGD-cell surface receptors, *Bioconjugate Chem.*, 2009, **20**(1), 87–94.

20 H. Cai, *et al.*, Engineering PLGA nano-based systems through understanding the influence of nanoparticle properties and cell-penetrating peptides for cochlear drug delivery, *Int. J. Pharm.*, 2017, **532**(1), 55–65.

21 R. Hassert, *et al.*, On-resin synthesis of an acylated and fluorescence-labeled cyclic integrin ligand for modification of poly(lactic-co-glycolic acid), *Chem. Biodiversity*, 2012, **9**(11), 2648–2658.

22 N. Bertrand, *et al.*, Mechanistic understanding of *in vivo* protein corona formation on polymeric nanoparticles and impact on pharmacokinetics, *Nat. Commun.*, 2017, **8**(1), 777.

23 O. Diou, *et al.*, RGD decoration of PEGylated polyester nanocapsules of perfluorooctyl bromide for tumor imaging: influence of pre or post-functionalization on capsule morphology, *Eur. J. Pharm. Biopharm.*, 2014, **87**(1), 170–177.

24 R. Wallbrecher, *et al.*, The stoichiometry of peptide-heparan sulfate binding as a determinant of uptake efficiency of cell-penetrating peptides, *Cell. Mol. Life Sci.*, 2014, **71**(14), 2717–2729.

25 E. Horisawa, *et al.*, Size-dependency of DL-lactide/glycolide copolymer particulates for intra-articular delivery system on phagocytosis in rat synovium, *Pharm. Res.*, 2002, **19**(2), 132–139.

26 B. Weiss, *et al.*, Nanoparticles made of fluorescence-labelled Poly(L-lactide-co-glycolide): preparation, stability, and biocompatibility, *J. Nanosci. Nanotechnol.*, 2006, **6**(9–10), 3048–3056.

27 https://www.federa.org/code-goed-gebruik.

28 P. Laverman, *et al.*, Microscopic localization of PEG-liposomes in a rat model of focal infection, *J. Controlled Release*, 2001, **75**(3), 347–355.

29 A. Loudet and K. Burgess, BODIPY dyes and their derivatives: syntheses and spectroscopic properties, *Chem. Rev.*, 2007, **107**(11), 4891–4932.

30 K. Trofymchuk, *et al.*, BODIPY-loaded polymer nanoparticles: chemical structure of cargo defines leakage from nanocarrier in living cells, *J. Mater. Chem. B*, 2019, **7**(34), 5199–5210.

31 A. R. El-Awady, *et al.*, Periodontal ligament fibroblasts sustain destructive immune modulators of chronic periodontitis, *J. Periodontol.*, 2010, **81**(9), 1324–1335.

32 B. Rath-Deschner, *et al.*, CXCL1, CCL2, and CCL5 modulation by microbial and biomechanical signals in periodontal cells and tissues-*in vitro* and *in vivo* studies, *Clin. Oral Investig.*, 2020, **24**(10), 3661–3670.

33 M. Y. Mahmoud, J. M. Steinbach-Rankins and D. R. Demuth, Functional assessment of peptide-modified PLGA nanoparticles against oral biofilms in a murine model of periodontitis, *J. Controlled Release*, 2019, **297**, 3–13.

34 I. A. Khalil, *et al.*, Octaarginine-modified multifunctional envelope-type nanoparticles for gene delivery, *Gene Ther.*, 2007, **14**(8), 682–689.

35 G. Kibria, *et al.*, Dual-ligand modification of PEGylated liposomes shows better cell selectivity and efficient gene delivery, *J. Controlled Release*, 2011, **153**(2), 141–148.

36 K. Takara, *et al.*, Size-controlled, dual-ligand modified liposomes that target the tumor vasculature show promise for use in drug-resistant cancer therapy, *J. Controlled Release*, 2012, **162**(1), 225–232.

37 H. Sun, *et al.*, Peptide-decorated polymeric nanomedicines for precision cancer therapy, *J. Controlled Release*, 2018, **290**, 11–27.